Water−Ethanol Mixtures at Different Compositions and Temperatures. A Dieletric Relaxation Study

P. Petong, R. Pottel, and U. Kaatze*

Drittes Physikalisches Institut, Georg-August-Universität, Bürgerstrasse 42-44, D-37073 Göttingen, Germany

Received: April 13, 2000

At eight temperatures T between 0 and 60 °C and at five mole fractions x_e of ethanol ($0 < x_e \leq 1$) the complex (electric) permittivity of ethanol/water mixtures has been measured as a function of frequency ν between 1 MHz and 24 GHz. At 25 °C the ethanol permittivities are completed by literature data for the frequency range 200 MHz to 90 GHz. The spectra for ethanol and for the ethanol/water mixtures are compared to permittivity spectra for water which, at some temperatures, are available up to 900 GHz. All spectra of the ethanol/water system can be well represented by the assumption of two relaxation regions. The relaxation time τ_1 of the dominating relaxation process varies between 4 ps ($x_e = 0$, 60 °C) and 310 ps ($x_e = 1$, 0 °C). The relaxation time τ_2 of the second relaxation process is smaller. Evaluation of the extrapolated low frequency ("static") permittivity yields a minium in the effective dipole orientation correlation of the ethanol/water system at $0.2 \leq x_e \leq 0.4$. In this composition range, other parameters also exhibit extrema, indicating a microheterogeneous structure of the mixtures and the existence of precritical concentration fluctuations. Interesting, the activation enthalpy $\Delta H_1^{\ddagger}$ and entropy $\Delta S_1^{\ddagger}$ of the dominating dielectric relaxation process also display a distinct maximum at around $x_e = 0.22$. These activation quantities have been obtained from Eyring plots of the relaxation time τ_1 at different mixture compositions. The relaxation parameters of the ethanol/water system are discussed in terms of a wait-and-switch model of dipole reorientation.

Introduction

Water as the most important liquid of the biosphere exhibits many eccentric properties due to its three-dimensional hydrogen-bond network.[1−5] The detailed knowledge of the liquid structure and of the microdynamics of water, therefore, is one of the outstanding problems in condensed-matter physics and in biophysics as well. Many investigations toward a better understanding of the unusual characteristics of water as liquid and solvent have been performed using selected organic solutes as probes.[6,7] Among the various components that have been added to water monohydric alcohols offer most favorable conditions for such studies owing to the amphiphilic nature of alcohol molecules. Alcohols interact strongly with water through hydrogen bonds and, depending on the number and steric arrangement of their alkyl groups, also through hydrophobic effects.

Dielectric relaxation spectrometry has proven a powerful tool, suitable to gain insights into the mechanisms of association and into the reorientational dynamics of dipolar liquids.[7−13] Despite several dielectric relaxation studies, however, the reorientational molecular motions in aqueous mixtures and in alcoholic systems are still insufficiently known. Alcohol/water mixtures[14−20] like alcohol/alcohol mixtures[16,18,21] normally behave as dielectrically homogeneous liquids, showing a relaxation frequency between the characteristic frequencies of the component relaxation processes. It is this intermediate relaxation frequency or relaxation time τ, respectively, which is of particular interest here. The relaxation time of monohydric alcohols and of some alcohol/water mixtures display a rather uniform behavior that appears to be predominantly governed by the density $\hat{\rho}$ of hydrogen-bonding sites.[22] In order to investigate the τ versus $\hat{\rho}$ relation more quantitatively, we recently performed dielectric relaxation measurements of ethanol/*n*-hexanol mixtures as a function of composition and temperature. Whereas in that study the hydrogen-bonding site content of ethanol has been reduced step by step on addition of the longer-chain alcohol, in this investigation $\hat{\rho}$ is increased by the addition of water.

Complex Permittivity Spectrometry

Principle of the Method. The complex (electric) permittivity

$$\epsilon(\nu) = \epsilon'(\nu) - i\epsilon''(\nu) \quad i^2 = -1 \tag{1}$$

of the liquids has been measured as a function of frequency ν by applying frequency domain techniques. Three methods have been used to cover the frequency range between 1 MHz and 24 GHz.

Quasistatic Input Impedance Measurements. At frequencies below 3 GHz the wavelength λ of the electromagnetic field within the liquids was sufficiently large to enable quasistatic approaches. The sample was contained in a coaxial line/circular waveguide transition. The diameter of the cell was sufficiently small (7 mm) to excite the waveguide section below the cut-off frequency ν_c of the TM_{01} field mode.[23]

Different lengths l (0 mm $\leq l \leq$ 40 mm) of the coaxial line part, filled with the liquid, have been used to match the cell capacity to the dielectric properties of the sample liquids and also to particular frequency ranges. A careful analysis of this cut-off type cells resulted in a rather simple equivalent circuit, indicating that, for each cell length l, four frequency-independent cell parameters have to be known for accurate measurements.[23] These parameters have been derived from calibration measurements, using the empty cell and the cell filled with water,

* Corresponding author.

10.1021/jp001393r CCC: $19.00
Published on Web 07/26/2000

acetone, and ethyl acetate as reference liquids. The input impedance of the cell has been determined as a function of frequency utilizing a computer-controlled network analyzer (HP 8753A), combined with a suitable reflection test set (HP 85044A).

Automated Transfer Function Measurements. In the frequency range from 5.3 GHz to 18 GHz, the transfer function of suitable double beam interferometers, constructed from wavequide components, has been recorded at continuously varying cell length by applying a computer-controlled mode of operation.[24] Two interferometers were used, one adjusted to the 5.3−8 GHz frequency band, and the other one to the 12.4−18 GHz band. The cells, essentially forming one branch of the respective interferometer, consisted of a circular cylindrical waveguide filled with the sample liquid. Another circular waveguide was immersed in the liquid. At each frequency of measurement, this waveguide was precisely shifted along the direction of wave propagation in order to probe the electromagnetic field within the cell at varying sample length. The off-balance interferometer transfer function measured thereby was fitted to an appropriate analytical expression to yield the propagation constant

$$\gamma = (\beta_c^{\,2} - \epsilon(\nu)\beta_o^{\,2})^{1/2} \qquad (2)$$

of the cell and thus the permittivity of the liquid. In eq 2 β_o and β_c denote the wavenumber in free space and the cut-off constant of the fundamental TM_{01} mode of the waveguide, respectively.

Nonautomated Propagating Wave Transmission Measurements. Between 20 and 24 GHz the attenuation coefficient of all sample liquids was sufficiently high to enable undisturbed propagating waves to be set up in the cell.[25,26] We used a waveguide double beam interferometer and a cell construction similar to that of the automated transfer function measurements. However, zero output signal of the interferometer has been manually adjusted to determine the complex constant of the wave within the liquid-filled cell.

Experimental Errors. Sample permittivity data obtained from cut-off cells of different length l and also from calibration routines with different reference liquids resulted in the following relative errors from the input impedance measurements: $\Delta\epsilon'/\epsilon' = 0.02$, $\Delta\epsilon''/\epsilon'' = 0.03$, $\nu < 5$ MHz; $\Delta\epsilon'/\epsilon' = 0.01$, $\Delta\epsilon''/\epsilon'' = 0.01$, 5 MHz $\leq \nu \leq 1$ GHz; $\Delta\epsilon'/\epsilon' = 0.05$, $\Delta\epsilon''/\epsilon'' = 0.07$, $\nu >$ 1 GHz. The errors in the permittivity data measured with both interferometer methods were $\Delta\epsilon'/\epsilon' = 0.02$ and $\Delta\epsilon''/\epsilon'' = 0.02$. In the complete range of measurements, the error in the determination of the frequency of the electromagnetic field was smaller than $\Delta\nu/\nu = 0.001$. The temperature of the sample was controlled to within 0.05 K and was measured with an error of 0.02 K.

Treatment of Dielectric Spectra. In order to analytically represent the frequency dependent permittivity of a sample, suitable relaxation spectral functions $R(\nu) = R'(\nu) - iR''(\nu)$, as detailed discussed below, have been fitted to the measured data. For this purpose, a Marquardt algorithm[27] has been used to minimize the reduced variance

$$\chi^2 = \frac{1}{N-P-1}\sum_{n=1}^{N}\left[\left(\frac{R'(\nu_n) - \epsilon'(\nu_n)}{\Delta\epsilon'(\nu_n)}\right)^2 + \left(\frac{R''(\nu_n) - \epsilon''(\nu_n)}{\Delta\epsilon''(\nu_n)}\right)^2\right] \qquad (3)$$

TABLE 1: Density (ρ) and Concentrations of Ethanol (c_e) and Water (c_w) of the Ethanol/Water Mixtures at Different Temperatures T and Mole Fractions x_e of Ethanol

$T \pm 0.05$, °C	$x_e = 0^{71}$	$x_e = 0.22$	$x_e = 0.36$	$x_e = 0.54$	$x_e = 0.76$	$x_e = 01$
			$\rho \pm 1.5$, mg/cm^3			
0	999.84	945.5	910.0	872.5	836.0	807.5
10	999.70	938.5	903.5	865.0	829.0	799.0
20	998.20	932.5	895.0	856.5	820.0	789.5
25	997.05	928.5	891.0	852.0	817.0	785.5
30	995.65	924.5	887.0	848.5	812.5	781.5
40	992.22	917.0	879.0	840.0	804.0	773.5
50	988.03	909.5	870.5	831.5	794.5	765.0
60	983.19	901.5	862.5	822.5	784.5	757.0
			$c_e \pm 0.02$, mol/L			
0	0	8.70	11.60	14.15	16.15	17.53
10	0	8.64	11.52	14.03	16.01	17.34
20	0	8.58	11.41	13.89	15.84	17.14
25	0	8.55	11.36	13.82	15.78	17.05
30	0	8.51	11.31	13.76	15.69	16.96
40	0	8.44	11.21	13.62	15.53	16.79
50	0	8.37	11.10	13.48	15.35	16.61
60	0	8.30	11.00	13.34	15.15	16.43
			$c_w \pm 0.02$, mol/L			
0	55.50	30.22	20.84	12.24	5.78	0
10	55.49	30.00	20.69	12.14	5.74	0
20	55.41	29.80	20.50	12.02	5.70	0
25	55.35	29.68	20.41	11.96	5.68	0
30	55.27	29.55	20.31	11.91	5.65	0
40	55.08	29.32	20.13	11.79	5.61	0
50	54.84	29.07	19.94	11.67	5.56	0
60	54.58	28.81	19.75	11.54	5.51	0

Herein ν_n, $n = 1, ..., N$, denotes the frequencies of measurement, P is the number of adjustable parameters of the model relaxation function R, and the inverse experimental errors $1/\Delta\epsilon'(\nu_n)$ and $1/\Delta\epsilon''(\nu_n)$ are used as weighing factors. The uncertainties in the parameter values of the relaxation function $R(\upsilon)$ have been obtained from additional runs in which the measured data were replaced by sets of pseudodata $\tilde{\epsilon}'(\nu_n) = \epsilon'(\nu_n) + r_n'\Delta\epsilon'(\nu_n)$ and $\tilde{\epsilon}''(\nu_n) = \epsilon''(\nu_n) + r_n''\Delta\epsilon''(\nu_n)$. Here r_n' and r_n'', $-1 \leq r_n', r_n'' \leq 1$, are random numbers.

Sample Liquids and Their Densities

Ethanol ("e"; >99%, Merck, Darmstadt, Germany) was used as delivered. Water was deionized by mixed bed ion exchange and distilled twice afterward. Mixtures with mole fraction $x_e = 0.22$, 0.36, 0.54, and 0.76 of ethanol have been obtained by weighing appropriate amounts of the constituents into suitable flasks. At eight temperatures T between 273.2 and 333.2 K the density ρ of the liquids has been determined with an accuracy of $\Delta\rho/\rho = 0.0015$ using an aerometer set. At 298.2 K the aerometer data have been verified by picnometric measurements. The densities of the sample liquids as well as the molar concentrations c_e and c_w of ethanol and water, respectively, are collected in Table 1. The concentrations have been calculated from the densities according to the relation

$$c_{e,w} = x_{e,w}\rho\,(x_eM_e + x_wM_w)^{-1} \qquad (4)$$

where M_e and M_w denote the molar weights of ethanol and water, respectively, and $x_e + x_w = 1$.

In Figure 1, at four temperatures, the densities ρ of the liquids are shown as a function of mole fraction x_e. Also presented is the graph of the ρ_{ideal} versus x_e relation at 60 °C which according to

$$\rho_{ideal} = ((M_e - M_w)x_e + M_w)((M_e/\rho_0^{\,e} - M_w/\rho_0^{\,w})x_e + M_w/\rho_0^{\,w})^{-1} \qquad (5)$$

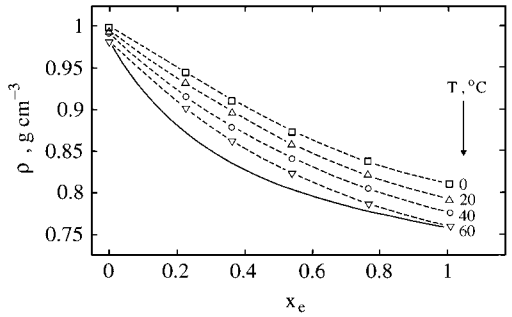

Figure 1. Density ρ of the ethanol/water mixtures at four temperatures T plotted versus the mole fraction x_e of ethanol. Dashed curves are drawn just to guide the eye. The full curve shows the density which at 60 °C is expected if ideal mixture behavior is assumed (eq 5).

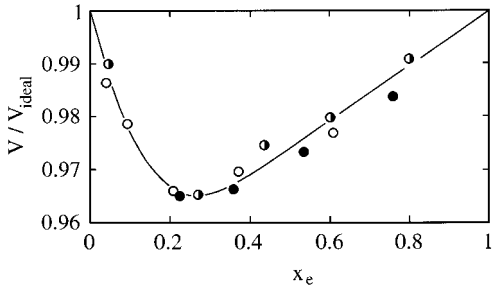

Figure 2. The volume ratio V/V_{ideal} of ethanol/water mixtures (eq 7) at 25 °C displayed versus mole fraction x_e of ethanol: ○;[28] ◑;[29] ●, our data.

is predicted for the ethanol/water mixtures if both constituents are assumed to maintain their molar volumes

$$V_0^{e,w}(T) = M_{e,w}/\rho_0^{e,w}(T) \tag{6}$$

Here subscript "0" refers to the pure constituents. Whereas the densities of the ethanol/*n*-hexanol system exhibit ideal mixture behavior,[21] a noticeable volume effect is found with the ethanol/water system. Obviously, it is the voluminous three-dimensional hydrogen bond structure of water which is predominantly affected by the second constituent. We calculated the volume ratio

$$\frac{V}{V_{ideal}} = \frac{1}{\rho}\frac{x_e M_e + x_w M_w}{x_e V_0^{e} + x_w V_0^{w}} \tag{7}$$

where V denotes the volume of a liquid of given mass and V_{ideal} the value predicted for the same mass of liquid if ideal mixture behavior is assumed. The V/V_{ideal} ratio at 25 °C is displayed as a function of mole fraction x_e in Figure 2. In fact, the V/V_{ideal} values decrease when small amounts of ethanol are added to water and display a relative minimum at $0.2 \le x_e \le 0.3$. Above $x_e = 0.3$, the volume ratio increases almost linearly with mole fraction of ethanol to reach $V/V_{ideal} = 1$ at $x_e = 1$. We shall have more detailed comment on this dependence upon the mixture composition in the Discussion.

Results and Discussion

Frequency-Dependent Permittivities of the Constituents. In Figure 3, the real parts $\epsilon'(\nu)$ and negative imaginary parts $\epsilon''(\nu)$ of the permittivity spectra at 20 °C are shown for both constituents. Our permittivity values for ethanol are completed with data by Chan from 0.2 to 20 GHz,[30] by Alison from 29 to 82 GHz,[31] and by Richards at 90 GHz.[32] There are some small differences between the Chan data and ours. Nevertheless, at ν < 10 GHz the ϵ' spectra can be well represented by a Debye type relaxation function $R_D(\nu)$ with discrete relaxation time. In Figure 3, the graph of this function, defined by[33]

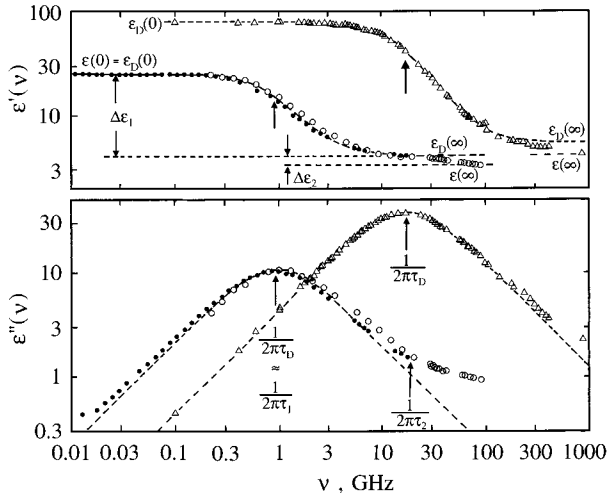

Figure 3. Real part ϵ' and negative imaginary part ϵ'' of the complex electric permittivity for water (△) and ethanol (○, ●) at 25 °C displayed as a function of frequency ν. Dashed curves show the low-frequency (dominating) relaxation ("1" in eq 9), the parameters of which almost agree with those from a fit of a Debye-type spectral function (eq 8) to the low-frequency part of the spectra: $\epsilon\ (0) = \epsilon(\infty) + \Delta\epsilon_1 + \Delta\epsilon_2 = \epsilon_D(0)$, $\tau_1 \approx \tau_D$; $\epsilon(\infty) + \Delta\epsilon_2 \approx \epsilon_D(\infty)$. Key: Δ;[38] O;[30−32] ●, our data.

$$R_D(\nu) = \epsilon_D(\infty) + \frac{\epsilon_D(0) - \epsilon_D(\infty)}{1 + i\omega\tau_D} \tag{8}$$

is shown by dashed curves. Here $\omega = 2\pi\nu$, $\epsilon_D(\infty)$ is the limiting permittivity as extrapolated from the dispersion region toward high frequencies (Figure 3), and $\epsilon_D(0)$ is the extrapolated low-frequency permittivity. At ν >10 GHz another dispersion ($d\epsilon'(\nu)/d\nu < 0$) emerges, indicating at least one further high-frequency relaxation. For monohydric alcohols a multiple Debye model with up to three discrete relaxation times has been reported in the literature.[17,20,21,32,34−37] To analytically represent the present spectra within the limits of error, it is sufficient to consider a two-Debye-term relaxation function

$$R(\nu) = \epsilon(\infty) + \frac{\Delta\epsilon_1}{1 + i\omega\tau_1} + \frac{\Delta\epsilon_2}{1 + i\omega\tau_2} \tag{9}$$

where $\epsilon(0) = \epsilon(\infty) + \Delta\epsilon_1 + \Delta\epsilon_2$. Toward high frequencies deviations of the measured $\epsilon''(\nu)$ values from the graph of eq 8 also clearly point at the existence of a second relaxation region. Deviations of the experimental $\epsilon''(\nu)$ values from the dashed curve at ν < 3 MHz may be taken to indicate some ionic impurities of the sample, leading to a conductivity contribution in the negative imaginary part of the spectrum,

$$\epsilon_\sigma''(\nu) = \sigma/(\epsilon_o\omega) \tag{10}$$

where σ in the specific electric (dc) conductivity of the liquid and ϵ_o denotes the electric field constant.

The permittivity data for water display a behavior very similar to those for ethanol, but the dispersion/dielectric loss regions are shifted to higher frequencies. The $\epsilon'(\nu)$ and $\epsilon''(\nu)$ values plotted in Figure 3 have been taken from a compilation of data from many laboratories.[38] At ν < 100 GHz, the complex dielectric spectrum of water can be well represented by a simple Debye-type spectral function (eq 8). However, if data at high frequencies are included,[39−46] noticeable deviations from a

TABLE 2: Parameters of the Debye-Type Relaxation Function (Eq 8) for Water at Different Temperatures T[a]

	refs for ϵ_D (0)				refs for τ_D, ps			refs for $\epsilon_D(\infty)$			
T, °C	47	38	32	IUPAC	47	38	32	47	38	32	$\bar{\epsilon}_D(\infty)$
0	87.91	87.79		87.37	17.67	17.57		5.7	4.5		5.7
5	85.83		85.84		14.91		14.30	5.7		6.2	5.7
10	83.92	83.88	83.91	83.91	12.68	12.50	12.55	5.5	5.4	6.1	5.6
15	82.05		82.03		10.83		10.86	6.0		6.0	5.6
20	80.21	80.15	80.16	80.16	9.36	9.40	9.38	5.6	5.3	5.7	5.6
25	78.36	78.38	78.34	78.36	8.27	8.28	8.29	5.2	5.5	5.6	5.5
30	76.56	76.58	76.57	76.57	7.28	7.35	7.35	5.2	5.8	5.3	5.4
35	74.87		74.84		6.50		6.59	5.1		5.7	5.3
40	73.18	73.17	73.16	73.16	5.82	5.84	5.82	3.9	5.3	5.3	5.2
50	69.89	69.89		69.90	4.75	4.80		4.0	4.6		4.8
60	66.70	66.70		66.79	4.01	3.85		4.2	2.5		4.2

[a] Data from three sets of permittivity values are given for comparison and also IUPAC static permittivity values. The $\bar{\epsilon}_D(\infty)$ values have been taken from a plot of the individual high-frequency permittivities, assuming a smooth temperature dependence.

single-relaxation-time behavior emerge, even though some of these high-frequency data are inconsistent with each other. Since we are interested in the microwave frequency range ($\nu < 100$ GHz) here and because permittivity data at $\nu > 100$ GHz exist at a few temperatures only, we represent the water dielectric spectrum by the Debye relaxation function (eq 8). The values for the parameters of this function at 0 °C $\leq T \leq$ 60 °C are collected in Table 2. For reasons of comparison, three sets of parameter values resulting from analyses of permittivity data between 1.1 and 58 GHz,[47] and between 0.1 and 70 GHz,[38] as well as between 1 and 90 GHz,[32] are given. Also included are the IUPAC standard static permittivity values ϵ_s resulting from low-frequency measurements.[38] The static permittivities and relaxation times from the different sets agree nicely. There exists a noticeable deviation only of the IUPAC static permittivity value at 0 °C from the others, and the difference between both τ_D values at 60 °C is rather large (4%). This latter difference is due to the fact that, at this temperature, the relaxation frequency (41 GHz) is located at the upper limit of the measuring ranges. Also at 5 °C the relaxation time from Richard's analysis (14.30 ps[32]) is smaller by 4.5% than the values of the other sets of parameter values. We regret having no explanation why this value does not fit.

As expected intuitively, the scatter in the $\epsilon_D(\infty)$ values is much higher. Due to the different high frequency limits in the three sets of permittivity data, there are considerable differences in the $\epsilon_D(\infty)$ values from the different evaluation procedures. Presuming a smooth $\bar{\epsilon}_D(\infty)$ versus T relation, we therefore estimated for the present measuring temperatures mean high-frequency permittivities $\bar{\epsilon}_D(\infty)$ to be used in the following discussion. These $\bar{\epsilon}_D(\infty)$ values are also presented in Table 2.

Permittivity Spectra of the Binary Mixtures. In Figure 4, the complex dielectric spectrum of the ethanol/water mixture of nearly equimolar composition is shown at the different temperatures of measurement. Within the frequency range covered in this study only one dispersion/dielectric loss region emerges. This finding supports the idea of a dielectrically almost homogeneous liquid. In particular, no special contributions are found in the spectra at the relaxation frequencies of the constituents. At 0 °C, the relaxation frequencies $(2\pi\tau_D)^{-1}$ and $(2\pi\tau_1)^{-1}$ of water and ethanol, respectively, are indicated by arrows in the diagram. Hence there do not seem to exist microphases in the mixture with relaxation times of water or ethanol. The same is true for the mixtures of other compositions. A careful analysis of the measured spectra of the ethanol/water mixtures, however, indicates that the frequency-dependent complex permittivites cannot be represented by a discrete relaxation time. In correspondence with ethanol, we therefore analyzed the spectra of the binary mixtures also in terms of the

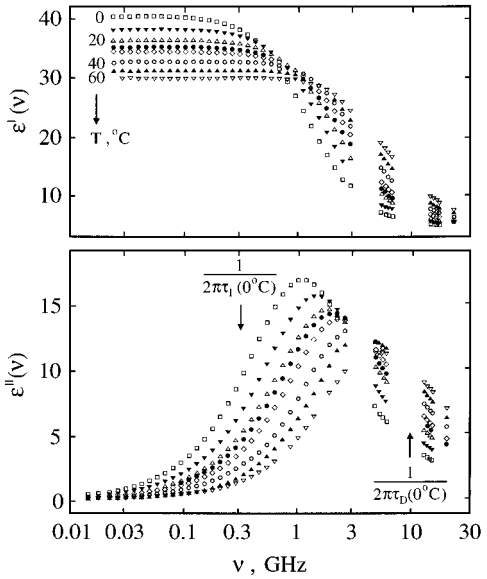

Figure 4. Real part ϵ' and negative imaginary part ϵ'' of the complex permittivity plotted versus frequency ν for the nearly equimolar ethanol/water mixture ($x_e = 0.54$) at the different temperatures of measurement. Arrows indicate the relaxation frequencies of the dominant relaxation term of the constituents at 0 °C.

double-Debye-relaxation model represented by eq 9. The values of the adjustable parameters of this relaxation function, as obtained from a nonlinear least-squares regression analysis of the measured spectra, are given in Tables 3 and 4. We only mention that, in the limited measuring range, relaxation spectral functions which are based on the assumption of a continuous relaxation time distribution are also appropriate. We found, for example, that the spectra can be adequately represented by the Davidson−Cole relaxation spectral function.[48]

Extrapolated Permittivites and Dipole Orientation Correlation. In Figure 5, the difference between the extrapolated high-frequency permittivity and the squared optical refractive index n^2 is shown. Refractive index data have been taken from the literature.[49−52] $\epsilon(\infty) - n^2 \approx 1.5$ for ethanol at all temperatures of measurement and the difference increases with the water content of the mixtures up to a (almost temperature independent) value of 2.5 at $x_e = 0.22$. Hence there exist electric polarization processes with characteristic frequencies in the far infrared and infrared region. The $\bar{\epsilon}_D(\infty) - n^2$ data for water show a tendency to decrease with temperature at $T > 30$ °C. However, the $\epsilon_D(\infty)$ values contain also contributions from the high-frequency relaxation process "2" ($(2\pi\tau_2)^{-1} > 100$ GHz; Figure 3) and do thus not directly compare to the $\epsilon(\infty)$ data for the other liquids.

TABLE 3: Extrapolated Static Permittivity $\epsilon(0)$ and Dispersion Steps $\Delta\epsilon_1$ and $\Delta\epsilon_2$ of the Relaxation Spectral Function Defined by Eq 9 for the Ethanol/Water Mixtures at Different Mole Fractions x_e and Temperatures T

$T \pm 0.05$, °C	$x_e = 0.22$	$x_e = 0.36$	$x_e = 0.54$	$x_e = 0.76$	$x_e = 1$
			$\epsilon(0) \pm 2\%$		
0	59.2	51.1	40.5	33.5	28.4
10	57.5	47.8	38.2	31.7	26.7
20	55.2	45.2	36.5	29.8	25.2
25	54.4	44.4	35.4	28.8	24.5
30	52.7	43.1	34.6	28.3	23.9
40	50.5	40.8	32.9	26.6	22.4
50	47.9	38.7	31.4	25.4	21.2
60	45.6	36.2	30.1	23.9	19.8
			$\Delta\epsilon_1$		
0	50.8 ± 1	45.0 ± 1	34.2 ± 0.7	28.2 ± 0.1	23.8 ± 0.1
10	49.8 ± 2	40.6 ± 0.6	31.3 ± 0.5	26.2 ± 0.1	22.2 ± 0.1
20	46.0 ± 1	35.1 ± 2	28.4 ± 0.3	24.2 ± 0.2	20.7 ± 0.1
25	44 ± 2	36.1 ± 3	27.2 ± 0.7	22.9 ± 0.3	20.0 ± 0.1
30	40 ± 3	29.3 ± 2	26.7 ± 0.6	22.6 ± 0.5	19.5 ± 0.1
40	35 ± 5	29 ± 2	24.8 ± 1	20.3 ± 0.6	18.1 ± 0.1
50	31 ± 5	25 ± 5	21.5 ± 0.5	19.0 ± 0.6	16.9 ± 0.1
60	27 ± 5	22 ± 5	18.7 ± 1	17.0 ± 0.7	15.6 ± 0.2
			$\Delta\epsilon_2$		
0	3.3 ± 0.8	1.2 ± 1	1.9 ± 0.5	1.4 ± 0.3	1.1 ± 0.5
10	3.1 ± 1	2.5 ± 1	2.4 ± 0.4	1.6 ± 0.3	1.1 ± 0.5
20	4.8 ± 2	5.5 ± 1	3.8 ± 0.4	1.8 ± 0.2	1.0 ± 0.5
25	6.1 ± 1	3.8 ± 2	4.2 ± 0.3	2.1 ± 0.3	1.1 ± 0.5
30	9 ± 3	9 ± 3	4.0 ± 0.5	2.0 ± 0.3	1.1 ± 0.5
40	12 ± 5	8 ± 3	4.4 ± 0.5	2.9 ± 0.3	1.0 ± 0.5
50	13 ± 5	9 ± 5	6.1 ± 0.7	3.0 ± 0.4	1.1 ± 0.5
60	15 ± 5	10 ± 5	7.7 ± 0.5	3.6 ± 0.3	1.1 ± 0.5

TABLE 4: Extrapolated High-Frequency Permittivity $\epsilon(\infty)$ and Relaxation Times τ_1 and τ_2 of the Spectral Function Defined by Eq 9 for Ethanol/Water Mixtures at Different Mole Fractions x_e of Ethanol and Temperatures T

$T \pm 0.05$, °C	$x_e = 0.22$	$x_e = 0.36$	$x_e = 0.54$	$x_e = 0.76$	$x_e = 1$
			$\epsilon(\infty)$		
0	5.1 ± 0.4	4.9 ± 0.1	4.4 ± 0.1	3.9 ± 0.1	3.5 ± 0.1
10	4.6 ± 0.2	4.7 ± 0.2	4.5 ± 0.1	3.9 ± 0.1	3.4 ± 0.2
20	4.4 ± 0.3	4.6 ± 0.3	4.3 ± 0.2	3.8 ± 0.1	3.5 ± 0.1
25	4.3 ± 0.2	4.5 ± 0.3	4.0 ± 0.1	3.8 ± 0.2	3.4 ± 0.2
30	4.0 ± 0.1	4.4 ± 0.2	3.9 ± 0.2	3.7 ± 0.2	3.3 ± 0.2
40	3.9 ± 0.2	4.3 ± 0.2	3.7 ± 0.2	3.4 ± 0.1	3.3 ± 0.3
50	4.3 ± 0.2	4.5 ± 0.3	3.8 ± 0.2	3.4 ± 0.2	3.2 ± 0.3
60	4.1 ± 0.3	4.2 ± 0.4	3.7 ± 0.1	3.3 ± 0.2	3.1 ± 0.3
			τ_1, ps		
0	81 ± 6	100 ± 5	131 ± 8	209 ± 2	310 ± 2
10	53 ± 4	75 ± 2	99 ± 7	156 ± 2	233 ± 1
20	38 ± 4	55 ± 3	80 ± 5	121 ± 1	184 ± 2
25	33 ± 4	45 ± 3	70 ± 6	108 ± 1	162 ± 2
30	28 ± 3	42 ± 4	60 ± 4	95 ± 2	143 ± 2
40	22 ± 10	32 ± 3	47 ± 3	80 ± 3	105 ± 1
50	17 ± 7	24 ± 10	40 ± 2	61 ± 2	82 ± 1
60	14 ± 6	20 ± 7	33 ± 2	49 ± 3	63 ± 1
			τ_2, ps		
0	19 ± 3	14 ± 3	20 ± 3	13 ± 2	6 ± 3
10	10 ± 4	14 ± 4	16 ± 2	12 ± 2	6 ± 3
20	8 ± 2	14 ± 3	16 ± 3	11 ± 1	8 ± 3
25	8 ± 3	9 ± 3	13 ± 2	12 ± 3	6 ± 3
30	8 ± 3	14 ± 4	11 ± 3	10 ± 2	7 ± 3
40	7 ± 5	9 ± 3	9 ± 2	11 ± 3	6 ± 3
50	7 ± 5	8 ± 5	10 ± 2	10 ± 1	5 ± 3
60	7 ± 5	8 ± 5	9 ± 2	9 ± 2	6 ± 3

Toward low frequencies, the $\epsilon'(\nu)$ values of the liquids at all temperatures and compositions are almost independent of frequency ν (Figures 3 and 4) so that the extrapolated static permittivity values are well defined by the measurements. As already aforementioned (Table 2), our $\epsilon(0)$ ($=\epsilon_D(0)$) values for water nicely agree with literature data. Within the limits of experimental error also the $\epsilon(0)$ values for ethanol agree with quasistatically measured data[50,53,54] so that the existence of any dispersion below our measuring range can be excluded. As expected on grounds of theoretical models,[9,55−57] the $\epsilon(0)$ values decrease monotonously with temperature and also with ethanol concentration. A higher ethanol concentration means a smaller concentration of dipolar groups here. In addition, the amount of the permanent electric dipole moment in the gaseous state is somewhat smaller for the ethanol molecule $\mu_e = 1.68$ D [21] than for the water molecule $\mu_w = 1.84$ D.[11]

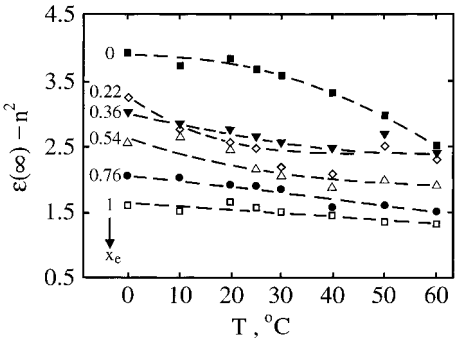

Figure 5. Difference between the extrapolated high-frequency permittivities $\epsilon(\infty)$ and the squared optical refractive index n^2 for the ethanol/water mixtures[49−52] of different mole fraction x_e shown as a function of temperature T. For water ($x_e = 0$) $\epsilon(\infty) = \bar{\epsilon}_D(\infty)$ is used here.

In general, the static permittivity of a mixture of different dipolar species is not just given by the amount of the molecular dipole moments and the concentrations of the dipolar species but also by dipole orientation correlation factors[58] and by a permittivity ϵ_∞ characterizing the polarizability of the liquid mixture well above the frequency range of permanent dipole moment relaxation. Strictly, water−water, water−ethanol, and ethanol−ethanol dipole orientation correlations have to be considered in the static permittivities of the present mixtures. Since we cannot derive three correlation factors from one permittivity value, we simply extend Fröhlich's theory for the static permittivity of a one-compound dipolar liquid[56] by introducing an effective dipole orientation correlation factor g_{eff}. The theoretical model then predicts

$$\epsilon(0) - \epsilon(\infty) = \frac{N_A}{3\epsilon_0 k_B T} \frac{3\epsilon(0)}{2\epsilon(0) + \epsilon_\infty} \left(\frac{\epsilon_\infty + 2}{3}\right)^2 g_{eff}(c_e \mu_e^2 + c_w \mu_w^2) \quad (11)$$

for the ethanol/water system. For the pure constituents g_{eff} equals the orientation correlation factor as originally introduced by Kirkwood.[58] In eq 11 N_A is Avogadro's number and k_B the Boltzmann constant.

Due to the large differences between the extrapolated high-frequency permittivity $\epsilon(\infty)$ and the squared optical refractive index n^2 (Figure 5), we do not know what ϵ_∞ values ($n^2 \le \epsilon_\infty \le \epsilon(\infty)$) are to be used in eq 11. This is an unfortunate situation because the g_{eff} data derived from eq 11 depend significantly upon ϵ_∞.[21,59] Since we are interested in an intercomparison of g_{eff} data at different temperatures and ethanol content rather than in absolute g_{eff} values, we nevertheless calculated effective dipole orientation correlation factors. We used $\epsilon_\infty = \epsilon(\infty)$ (Table 4) for all liquids containing ethanol. In order to use a corresponding high-frequency permittivity $\epsilon(\infty) = \epsilon_D(\infty) - \Delta\epsilon_2$ for water, we took $\Delta\epsilon_2 = 1.3$ at 20 °C (Figure 3) and we estimated the $\Delta\epsilon_2$ values at the other temperatures using the T

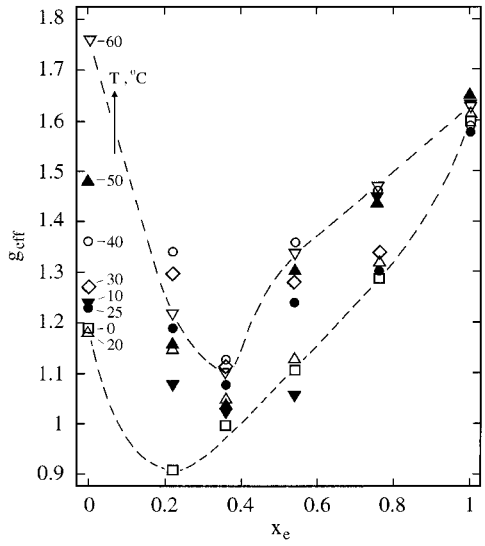

Figure 6. Effective orientation correlation factor g_{eff} (eq 11) of the ethanol/water system at the different temperatures of measurement displayed versus mole faction x_e of ethanol.

dependence of eq 11: $\Delta\epsilon_2(T) = \Delta\epsilon_2(293\text{ K})\cdot 293\text{ K}/T$. The g_{eff} data obtained thereby are displayed in Figure 6. Due to the variance in the ϵ_∞ parameter of eq 11, the values of these effective dipole orientation correlation factors and their dependence upon temperature should not be overemphasized. The conclusion may nevertheless be drawn that, in the temperature range of measurements, the orientation correlation of the molecular electric dipole moments of the ethanol/water system adopts a minimum at $0.2 \le x_e \le 0.4$.

High-Frequency Relaxation: Wait-and-Switch Model. The relaxation frequency $(2\pi\tau_2)^{-1}$ of the ethanol spectrum corresponds with the upper limit of our measuring range. There is thus a considerable experimental error in the parameters of the high-frequency relaxation term (Tables 3 and 4). Likewise uncertain are the parameter values of this term at high water content ($x_e = 0.22$ and 0.36) and at high temperatures ($T \ge 40$ °C), where the difference between the relaxation times τ_1 and τ_2 is small and, therefore, a clear subdivision of the measured spectra into two relaxation terms is hardly possible.

Within the limits of experimental error, the relaxation time τ_2 of the ethanol spectrum is independent of temperature (5 ps $\le \tau_2 \le$ 9 ps) (Table 4). It exceeds the relaxation time of the high-frequency water relaxation by about 1 order of magnitude ($\tau_2 \approx 1$ ps; Figure 3). The relaxation amplitude $\Delta\epsilon_2$ of the ethanol spectrum is also independent of T, and its value ($\Delta\epsilon_2 \approx 1.1$) is almost in agreement with that of the water spectrum at 20 °C ($\Delta\epsilon_2 = 1.3$; Figure 3).

This is an unexpected finding because of the different structures of both polar liquids. Whereas water molecules form a three-dimensional random hydrogen bond network well above the percolation threshold,[60−62] predominantly chainlike H-bonded structures exist in alcohols. The relaxation times (7 ps $\le \tau_2 \le$ 20 ps) and relaxation amplitudes ($1.2 \le \Delta\epsilon_2 \le 16$) of the mixtures are larger than the corresponding parameters of the constituents, indicating that ethanol and water substantially affect each other's high-frequency relaxation.

Recently, we have shown that the relaxation properties of alcohols and of alchohol/alcohol mixtures may be qualitatively discussed in a consistent way in terms of a wait-and-switch model.[21] This model is based on computer simulation studies of water,[60−64] but an analogous view of the dipole reorientational motions in alcohols had been already suggested in 1962 by Sagal.[65] It is now well established that the hydrogen bond strength of water and alcohols fluctuates rapidly. The characteristic correlation times τ_{HB} of these fluctuations are on the order of 0.1−1 ps,[60,61] corresponding with frequencies $(2\pi\tau_{HB})^{-1} > 150$ GHz. However, large-angle orientational motions of the molecular dipoles are controlled by larger correlation times, due to the necessity of two preconditions which have to be simultaneously fulfilled for dipole reorientational motions through significant angles. First, an additional neighbor, for example, the fifth neighbor in the random tetrahedral hydrogen network of water,[63] has to be present tending to flatten the angular distribution of rotational barriers. Hence, it reduces the activation enthalpy in the reorientational motion of the molecular dipole. Second, in addition to the activation mechanism, this or an additional neighbor molecule has to offer the possibility for the formation of a new H-bond. In water, at room temperature, it takes 10 ps until such favorable conditions for a dipole reorientation of a given molecule exist (Table 2). As compared to other associating liquids, this period is nevertheless short, due to the rather high amount of 5-fold and even 6-fold coordinated molecules in liquid water.[64] Without doubts, however, the dielectric relaxation times of water and alcohols are largely controlled by the period for which the molecules have to wait until both preconditions for an orientational motion are fulfilled. The reorientation process itself resembles a switching. It occurs within the short period of 0.1 ps.[60,61]

Within the framework of this wait-and-switch model, the high-frequency relaxation of alcohols has been attributed to the reorientational motions of single-H-bonded dipolar groups. In ethanol, according to computer simulation studies,[66] 14.7% of the −OH groups are involved in one hydrogen bond only. Due to this rather small content of single-bonded groups, the relaxation amplitude $\Delta\epsilon_2$ is small. As a result of the high concentration of sites in which double-H-bonded −OH groups offer an additional neighbor for a new hydrogen bond (77%[66]), the period is short for which a single-H-bonded −OH group has to wait for the switching into a new direction. Consequently, the dielectric relaxation time τ_2 is small. Similar arguments might be given for the very small amount of single-bonded molecules in water. However, our present knowledge of the high-frequency relaxation in water is too incomplete to allow for definite conclusions.

Following this assignment of relaxation terms to molecular reorientation mechanisms, the content of single-H-bonded dipolar groups or molecules in the ethanol/water mixtures appear to be higher than in the pure constituents. This is particular true at high water concentrations where $\Delta\epsilon_2$ values on the order of 10 exist. Roughly, in conformity with the idea of a wait-and-switch mechanism, the relaxation time in the mixtures is also larger than in the constituents. We assume these higher values to reflect the reduced number density of sites offering an additional neighbor for the formation of a new hydrogen bond. Since the τ_2 values of the mixtures (Table 4) are on the order of the low-frequency (dominating) relaxation time τ_D of water (Table 2), it might be argued that microphases with almost unaltered water relaxation times exist in the binary liquids. However, due to the high ethanol concentration in all mixtures considered in this investigation ($c_w/c_e < 4$ even at $x_e = 0.22$) the existence of water regions with unaffected relaxation properties appears to be unlikely.

In Figure 7, the relative contribution $\Delta\epsilon_2/(\Delta\epsilon_1 + \Delta\epsilon_2)$ of the high-frequency relaxation to the total dispersion step $\Delta\epsilon_1 + \Delta\epsilon_2 = \epsilon(0) - \epsilon(\infty)$ at 25 °C is shown as a function of the concentration c_μ of dipolar molecules. In addition to the data

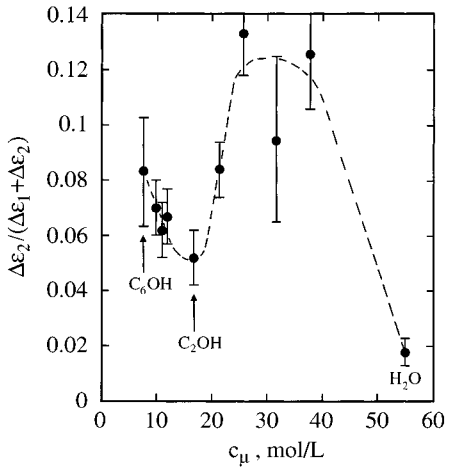

Figure 7. Relative contribution $\Delta\epsilon_2/(\Delta\epsilon_1 + \Delta\epsilon_2) = \Delta\epsilon_2/(\epsilon(0) - \epsilon(\infty))$ of the high-frequency relaxation to the total relaxation amplitude at 25 °C shown as a function of the concentration c_μ of dipolar molecules for the ethanol/water system and also for mixtures[21] of ethanol (C_2OH) with hexanol (C_6OH).

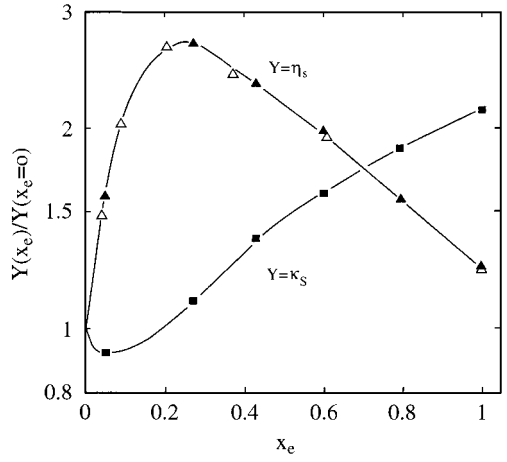

Figure 8. Viscosity ratio $\eta_s(x_e)/\eta_s(0)$ (△,[28] ▲;[29] $\eta_s(0) = 0.8903 \times 10^{-3}$ Pa·s) and adiabatic compressibility ratio $\kappa_s(x_e)/\kappa_s(0)$ (■;[29] $\kappa_s(0) = 4.479 \times 10^{-10}$ m^2 N^{-1}) for the ethanol/water mixtures at 25 °C plotted versus mole fraction x_e of ethanol.

for the ethanol/water system ($c_\mu = c_e + c_w$), data for hexanol/ethanol mixtures ($c_\mu = c_{hex} + c_e$) are also presented. The relative contribution to the dispersion step strongly increases from about 2% to 12% when ethanol is added to water. This substantial change in the dielectric relaxation properties corresponds with the change in the V/V_{ideal} ratio (Figure 2) at $x_e < 0.2$ and also with the reduction in the adiabatic compressibility κ_s of the ethanol/water system at small x_e (Figure 8). The compressibilities according to

$$\kappa_s = \rho^{-1} c_s^{-2} \tag{12}$$

have been derived from the densities and from sound velocity data c_s at 1 MHz.[29] Addition of ethanol to water at small x_e obviously leads to a less voluminous and less compressible liquid structure, characterized by a rather high content of single-H-bonded dipolar −OH groups and/or water molecules. At small x_e, it is an obvious suggestion to assume clathratelike hydration structures around the hydrophobic hydrocarbon group of ethanol molecules.[7,22]

Toward pure ethanol ($c_\mu = c_e = 17.05$ mol/L; Figure 7) the $\Delta\epsilon_2/(\Delta\epsilon_1 + \Delta\epsilon_2)$ values of the ethanol/water system decrease, indicating that a smaller amount of dipolar groups or molecules

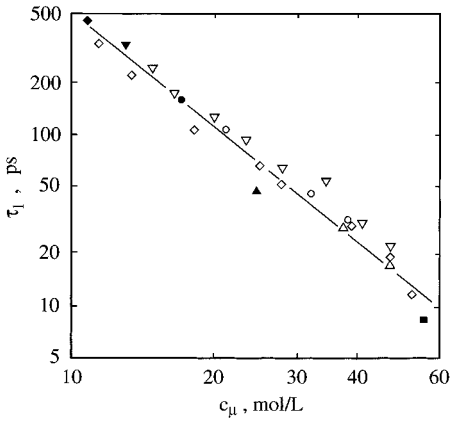

Figure 9. Relaxation time τ_1 of the dominating relaxation term as a function of the concentration c_μ of dipolar molecules for mixtures of water with methanol (△[17]), ethanol (○), 2-propanol (▽[17]), and *tert*-butyl alcohol (◇[20]). Full symbols denote the pure alcohols, respectively, and water is indicated by a full quad. Since another relaxation model had been applied to the series of *tert*-butyl alcohol/water spectra, the relaxation time $\hat{\tau}$ corresponding with the frequency $\hat{\nu} = (2\pi\hat{\tau})^{-1}$ of the maximum in the $\epsilon''(\nu)$ curve is given here.

is only single-H-bonded. Obviously, at a low water content predominantly chainlike structures, as characteristic for alcohols, exist. In contrast to the mixture behavior of ethanol and water, the relative contribution of the high-frequency relaxation to the total dispersion step of the hexanol/ethanol mixtures varies monotonously with mixture composition. This concentration dependence is in conformity with the ideal mixture properties of the alcohol/alcohol system as reflected by its density data.[21]

Low-Frequency Relaxation: Precritical Behavior. According to our discussion of characteristic frequency ranges in the ethanol/water dielectric spectra, dipole reorientational motions of non-H-bonded −OH groups or water molecules are assumed to contribute to the extrapolated high-frequency permittivity $\epsilon(\infty)$ ($> n^2$; Figure 5) while dipole reorientations of single-H-bonded dipolar groups and molecules are reflected by the high-frequency relaxation term. Consequently, the low-frequency (dominating) relaxation must be due to switching of double-H-bonded −OH groups and of multiply-hydrogen-bonded water molecules into a new dipole direction. Because there are high concentrations of double- or multiply-bonded molecules, the dispersion step $\Delta\epsilon_1$ of the low-frequency process is large. Since there exists only a comparatively small concentration of sites that are capable to act as an additional neighbor in the formation of a new bond, the relaxation time τ_1 is larger than τ_2. As expected for a wait-and-switch mechanism in which the relaxation time is controlled by the "wait" period, τ_1 decreases with increasing concentration c_μ of hydrogen-bonding offering molecules (Figure 9).

As illustrated by Figure 10, the temperature dependence of τ_1 follows an Eyring-type behavior of an activated jump mechanism[1]

$$\tau_1 = \frac{h}{k_B T} C_f \exp(\Delta G_1^{\ddagger}/RT) \tag{13}$$

Here h is Planck's constant, C_f denotes a configurational factor almost independent of T, $G_1^{\ddagger} = \Delta H_1^{\ddagger} - T\Delta S_1^{\ddagger}$ is the Gibbs free energy of activation of relaxation "1", and $R = k_B N_A$ is the gas constant. Most interesting, the activation enthalpy $\Delta H_1^{\ddagger}$ and the activation entropy $\Delta S_1^{\ddagger}$ exhibit relative maxima (Figure 11) in that composition range ($0.2 < x_e < 0.3$) in which the shear viscosity η_s adopts a relative maximum (Figure 8). Also

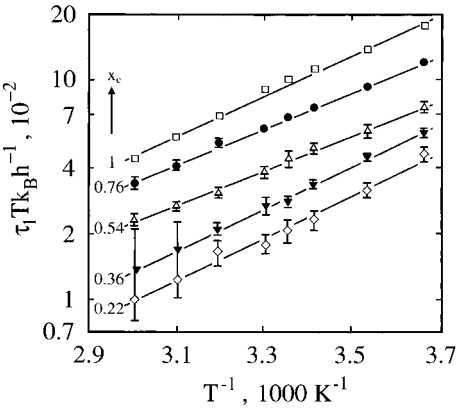

Figure 10. Eyring plot for the relaxation time τ_1 of the low-frequency (dominating) process of the ethanol/water mixtures.

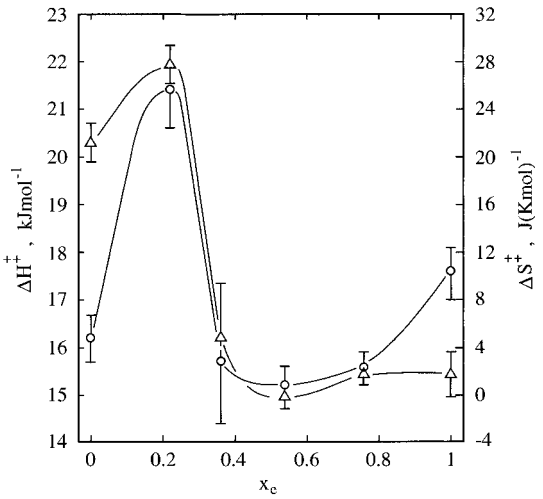

Figure 11. Activation enthalpy $\Delta H_1^{\ddagger}$ and entropy $\Delta S_1^{\ddagger}$ of the dominating dielectric relaxation process of ethanol/water mixtures shown as a function of mole fraction x_e of ethanol.

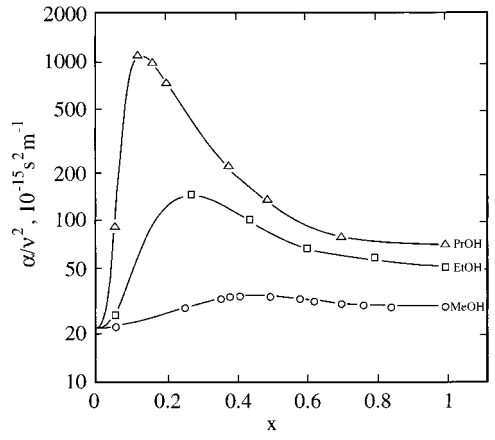

Figure 12. Frequency-normalized ultrasonic attenuation coefficient at $\nu = 1.5$ MHz and 25 °C semilogarithmically plotted as a function of mole fraction x of alcohol for mixtures of water with methanol (○), ethanol (□), and *n*-propanol (△).[29]

in this composition range, the frequency-normalized ultrasonic attenuation coefficient at low frequencies displays a maximum (Figure 12). The dependence of the concentration of maximum ultrasonic absorption and of the maximum value itself from characteristics of the alcohol, as well as a systematic analysis of sonic attenuation spectra of short-chain alcohol mixtures with water, suggest a tendency toward a microheterogeneous "precritical" structure of the liquids. Within the series of unbranched normal alcohols, this tendency increases with the length of the hydrophobic part of the molecules.[29,67] The ultrasonic spectra of ethanol/water mixtures yield a fluctuation correlation length ξ which peaks in the range $0.2 < x_e < 0.3$ but its maximum value is still small ($\xi = 2.9$ Å at $x_e = 0.27$ [67]). As a result of the maxima in both ξ and η_s the mutual diffusion coefficient[68,69]

$$D = k_B T/(6\pi\eta_s\xi) \qquad (14)$$

adopts a minimum value in this concentration range ($D = 3.2 \times 10^{-10}$ m^2 s^{-1} at $x_e = 0.27$; $D = 10 \times 10^{-10}$ m^2 s^{-1} at $x_e = 0.79$).[67] Despite of this effect of precritical slowing down, due to the rather high equilibrium concentration of single-H-bonded alcoholic −OH groups and water molecules, the probability for a phase "1" molecule to form a new hydrogen bond is high at $0.2 < x_e < 0.3$. The activation entropy $\Delta S_1^{\ddagger}$ of the dominating dielectric relaxation adopts a maximum in this composition range. The enhancement of the reorientational mobility resulting thereby is largely compensated by the maximum in the $\Delta H_1^{\ddagger}$ values. Structures with particularly high activation enthalpies are formed in a wide range of ethanol/water mixture compositions (Figure 11). In this context, it is interesting to notice that the formation of precritical microheterogeneous liquid structures in binary aqueous systems is mainly controlled by the hydrophobic part of the nonaqueous constituents.[67]

Acknowledgment. Financial support by the Deutsche Forschungsgemeinschaft is gratefully acknowledged.

References and Notes

(1) Eisenberg, D.; Kauzmann, W. *The Structure and Properties of Water;* Clarendon: Oxford, U.K., 1969.
(2) Franks, F., Ed. *Water, a Comprehensive Treatise, Vol. 1*: *The Physics and Physical Chemistry of Water*; Plenum: New York, 1972.
(3) Luck, W. A. P., Ed. *Structure of Water and Aqueous Solutions*; Verlag Chemie, Physik Verlag: Weinheim, Germany, 1974.
(4) Alfsen, A.; Berteaud, A. J., Eds. *L'eau et les systèmes biologiques*; (Water and Biological Systems); Editions due CNRS: Paris, 1976.
(5) Franks, F.; Mathias, S., Eds. *Biophysics of Water*; Wiley: New York, 1982.
(6) Franks, F. *Water, a Comprehensive Treatise, Vol. 2: Water in Crystalline Hydrates, Aqueous Solutions of Simple Nonelectrolytes;* Plenum: New York, 1973.
(7) Kaatze, U. *J. Solution Chem.* **1997**, *26*, 1049.
(8) Daniel, V. V. *Dielectric Relaxation*; Academic Press: London, 1967.
(9) Hill, N. E.; Vaughan, W. E.; Price, A. H.; Davies, M. *Dielectric Properties and Molecular Behaviour*; Van Nostrand Reinhold: London, 1969.
(10) Davies, M. *Dielectric and Related Molecular Process*; The Chemical Society: London, 1972, 1975, 1977; Vols. 1−3.
(11) Hasted, J. B. *Aqueous Dielectrics*; Chapman and Hall: London, 1973.
(12) Grant, E. H.; Sheppard, R. J.; South, G. P. *Dielectric Behaviour of Biological Molecules in Solution*; Clarendon: Oxford, U.K., 1978.
(13) Pethig, R. *Dielectric and Electronic Properties of Biological Material*; Wiley: Chichester, U.K., 1979.
(14) Perl, J. P.; Wasan, D. T.; Winsor, P.; Cole, R. H. *J. Mol. Liq.* **1984**, *28*, 103.
(15) Gestblom, B.; Sjöblom, J. *Acta Chem. Scand. A* **1984**, *38*, 47, 575.
(16) Mashimo, S.; Kuwabara, S.; Yagihara, S.; Higasi, K. *J. Chem. Phys.* **1989**, *90*, 3292.
(17) Kaatze, U.; Schäfer, M.; Pottel, R. *Z. Phys. Chem. Neue Folge* **1989**, *165*, 103.
(18) Mashimo, S.; Umehara, T.; Redlin, H. *J. Chem. Phys.* **1991**, *95*, 6257.
(19) Barthel, J.; Buchner, R. *Pure Appl. Chem.* **1991**, *63*, 1473.
(20) Kaatze, U.; Schumacher, A.; Pottel, R. *Ber. Bunsenges. Phys. Chem.* **1991**, *95*, 585.
(21) Petong, P.; Pottel, R.; Kaatze, U. *J. Phys. Chem. A.* **1999**, *103*, 6114.
(22) Kaatze, U.; Pottel, R. *J. Mol. Liq.* **1992**, *52*, 181.
(23) Göttmann, O.; Kaatze, U.; Petong, P. *Meas. Sci. Technol.* **1996**, *7*, 525.

(24) Kaatze, U.; Pottel, R.; Wallusch, A. *Meas. Sci. Technol.* **1995**, *6*, 1201.
(25) Pottel, R. *Ber. Bunsen-Ges. Phys. Chem.* **1965**, *69*, 363.
(26) Kaatze, U.; Giese, K. *J. Mol. Liq.* **1987**, *36*, 15.
(27) Marquardt, D. W. *J. Soc. Ind. Appl. Math.* **1963**, *2*, 2.
(28) Covington, A. K., Dickinson, T., Eds. *Physical Chemistry of Organic Solvent Systems*; Plenum: New York, 1973.
(29) Brai, M.; Kaatze, U. *J. Phys. Chem.* **1992**, *96*, 8946.
(30) Chan, T. Y. 1990, data quoted in ref 32.
(31) Alison, J. M. Dissertation, University of London, London, 1991.
(32) Richards, M. G. M. Dissertation, King's College London, London, 1993.
(33) Debye, P. *Polare Molekeln* (Polar Molecules); Hirzel: Leipzig, Germany, 1929.
(34) Garg, S. K.; Smyth, C. D. *J. Phys. Chem.* **1965**, *69*, 1294.
(35) Crossley, J. *Adv. Mol. Relax. Processes* **1970**, *2*, 69.
(36) Jakusch, E.; Sobczyk, L. Reference 10, Vol. 3, p 108.
(37) Szwarnowski, S. Dissertation, University of London, London, 1979.
(38) Lamkaouchi, K. Dissertation, L'Universite Bordeaux I, Bordeaux, 1992. Ellison, W. J.; Lamkaouchi, K.; Moreau, J. M. *J. Mol. Liq.* **1996**, *68*, 171.
(39) Goronina, K. A.; Belov, R. K.; Sorokina, E. P. *Izv. Vyssh. Ucheb. Zaved. Radiofiz.* **1966**, *9*, 975.
(40) Davies, M.; Pardoe, G. W. F.; Chamberlain, J.; Gebbie, H. A. *Trans. Faraday Soc.* **1970**, *66*, 273.
(41) Downing, H. D.; Williams, D. *J. Geophys. Res.* **1975**, *80*, 1656.
(42) Afsar, M. N.; Hasted, J. B. *J. Opt. Soc. Am.* **1977**, *67*, 902.
(43) Afsar, M. N.; Hasted, J. B. *Infrared Phys.* **1978**, *18*, 835.
(44) Blue, M. D. *J. Geophys. Res.* **1980**, *85*, 1101.
(45) Hasted, J. B.; Husain, S. K.; Frescura, F. A. M.; Birch, J. R. *Infrared Phys.* **1987**, *27*, 11.
(46) Manabe, T.; Liebe, H. J.; Hufford, G. A. *IEEE Conf. Dig. 12th Conf. IR Millimetre Waves* **1987**, 220.
(47) Kaatze, U. *J. Chem. Eng. Data* **1989**, *34*, 371.
(48) Davidson, D. W.; Cole, R. H. *J. Chem. Phys.* **1950**, *18*, 1417.
(49) D'Ans, J., Lax, E., Eds. *Taschenbuch für Chemiker und Physiker* (Handbook for Chemists and Physicists), 2nd Ed.; Springer: Berlin, 1949.
(50) Hellwege, K.-H., Hellwege, A. M., Eds.; Landolt-Börnstein, New Series, Part 2, 6th Ed.; Springer: Berlin, 1971.
(51) Ortega, J. *J. Chem. Data* **1982**, *27*, 312.
(52) Steger, H. Dissertation, Universität Regensburg, Regensburg, Germany, 1991.
(53) Buckley, F.; Maryott, A. A. *Tables of Dielectric Dispersion Data for Pure Liquids and Dilute Solutions*; NBS Circular 589; National Bureau of Standards: Washington, DC, 1958.
(54) Achadov, Y. Y. *Dielectric Properties of Binary Solutions;* Pergamon: Oxford, U.K., 1981.
(55) Brown, W. F. In *Encyclopedia of Physics*; Flügge, S., Ed.; Springer: Berlin, 1956; Vol. 17.
(56) Fröhlich, H. *Theory of Dielectrics;* Clarendon: Oxford, U.K., 1958.
(57) Boettcher, C. J. F. *Theory of Electric Polarization. 1. Dielectrics in Static Fields;* Elsevier: Amsterdam, 1973.
(58) Kirkwood, J. G. *J. Chem. Phys.* **1939**, *7*, 911.
(59) Hill, N. E. *J. Phys. C: Solid State Phys.* **1979**, *3*, 238.
(60) Tanaka, H.; Ohmine, I. *J. Chem. Phys.* **1987**, *87*, 6128.
(61) Ohmine, I.; Tanaka, H.; Wolynes, P. G. *J. Chem. Phys.* **1988**, *89*, 5852.
(62) Sciortino, F.; Fornili, S. L. *J. Chem. Phys.* **1989**, *90*, 2786.
(63) Geiger, A.; Mausbach, P.; Schnitker, A. In *Water and Aqueous Solutions;* Neilson, G. W., Enderby, J. E., Eds.; Hilger: Bristol, U.K., 1986.
(64) Sciortino, F.; Geiger, A.; Stanley, H. E. *J. Chem. Phys.* **1992**, *96*, 3857.
(65) Sagal, M. W. *J. Chem. Phys.* **1962**, *36*, 2437.
(66) Jørgensen, W. L. *J. Chem. Phys.* **1986**, *90*, 1276.
(67) Rupprecht, A.; Kaatze, U. *J. Phys. Chem.* **1999**, *103*, 6485.
(68) Kawasaki, K. *Ann. Phys.* **1970**, *61*, 1.
(69) Ferrell, R. A. *Phys. Rev. Lett.* **1970**, *24*, 1169.